

# Origin of Low-Energy Peaks in the Ti-K XANES Spectra of SrTiO<sub>3</sub> and CaTiO<sub>3</sub>

Masaki FUJITA<sup>a</sup>, Hirohide NAKAMATSU<sup>b</sup>, Sunao SUGIHARA<sup>c</sup>,  
Jun-ichi AIHARA<sup>a</sup> and Rika SEKINE<sup>a,\*</sup>

<sup>a</sup>Department of Chemistry, Faculty of Science, Shizuoka University  
836 Ohya, Shizuoka 422-8529, Japan

<sup>b</sup>Institute for Chemical Research, Kyoto University  
Gokasho, Uji, Kyoto 611-0011, Japan

<sup>c</sup>Department of Materials Science and Ceramic Technology, Shonan Institute of Technology  
1-1-25 Tsujido Nishikaigan, Fujisawa 251-8511, Japan

\*e-mail: [scrseki@ipc.shizuoka.ac.jp](mailto:scrseki@ipc.shizuoka.ac.jp)

(Received: August 11, 2003; Accepted for publication: November 5, 2003; Published on Web: December 24, 2003)

Low-energy parts of the Ti-K XANES spectra for SrTiO<sub>3</sub> and CaTiO<sub>3</sub> consist of a main peak and pre-edge peaks B and C. We made a characterization of these peaks using the DV X $\alpha$  cluster model combined with L<sup>2</sup> continuum wave functions. This approach with a [TiO<sub>6</sub>M<sub>8</sub>(TiO<sub>5</sub>)<sub>6</sub>M<sub>24</sub>]<sup>20+</sup> model cluster (M=Sr or Ca) was successful in reproducing the relative positions and intensities of the low-energy peaks. It was found that transitions of the titanium 1s electron to *p*-type atomic orbitals (AOs) of the same atom are responsible for all these peaks. In general, *p*-type atomic orbitals (AOs) of the central titanium atom are mixed with various AOs of nearby atoms in the model cluster. Thus, the origin of main and pre-edge peaks for typical perovskite-type titanates has been elucidated consistently within a single theoretical framework.

**Keywords:** XANES, Pre-edge peaks, Strontium titanate, Calcium titanate, DV-X $\alpha$  method

## 1 Introduction

X-ray absorption near-edge structure (XANES) and extended X-ray absorption fine structure (EXAFS) analyses provide element-sensitive methods for short-range atomic structure determinations in various chemical species [1]. In particular, XANES has been used as a fingerprint spectrum of a complex chemical species. However, it is not easy to interpret such spectra in band-theoretical or molecular orbital terms. We are in urgent need of developing practical methods for the assignments of X-ray absorption bands. Perovskite-type ferroelectric double oxides provide good candidates for theoretical or computational XANES analysis [2–6].

Ravel *et al.* [2, 3] measured the XANES spectra of several titanate perovskites and observed that some common pre-edge peaks appear on the low-energy side of the main peak. In order to characterize these absorption peaks, calculations of transition energies and oscillator strengths are necessary. For this purpose, theoretical XANES spectra have often been obtained using a multi-

ple scattering (MS) method with appropriate clusters of finite size. Bouldin *et al.* [4] and Ankudinov *et al.* [5] employed this method to reproduce the XANES spectra of BaTiO<sub>3</sub> and PbTiO<sub>3</sub>, respectively. Vedrinskii *et al.* analyzed the XANES spectra of several perovskite-type titanates using a modified MS method [6]. Wu *et al.* simulated the Ti-K XANES data on titanium oxides using full MS theory [7].

Another theoretical approach to XANES spectra is based on molecular orbital (MO) theory. MO-based methods, such as the discrete variational (DV) X $\alpha$  cluster method, are of potential utility in effectively reproducing XANES features because atomic orbitals (AOs) used as basis functions are localized at constituent atoms [8–14]. In this paper, we attempted to establish the assignments of low-energy XANES peaks for two typical titanates, SrTiO<sub>3</sub> and CaTiO<sub>3</sub>, using the DV X $\alpha$  cluster method [15]. This method has been applied successfully to the analysis of XANES spectra for such species as SF<sub>6</sub>, N<sub>2</sub>, and CeO<sub>2</sub> [8–14].

## 2 Computational Method

The DV X $\alpha$  method [15] can be extended to include the L<sup>2</sup> method [16, 17], in which continuum wave functions are discretized in finite sets of square integrable (L<sup>2</sup>) basis functions. A sufficiently large basis set is used to construct quasi-bound wave functions in a limited space where the integration for the oscillator strength is performed [18]. A linear combination of many bound and L<sup>2</sup> continuum atomic wave functions [18] is then used to express the continua. A so-called X $\alpha$  potential was used which is much more realistic than the muffin-tin potential. The effect of hole formation on the X-ray absorption spectra was explicitly included in the self-consistent charge density calculation [8–14].

Our basis set consists of AOs in the ranges from 1s to 5d for calcium, titanium and strontium, and from 1s to 4f for oxygen, and *s*-, *p*-, *d*-, and *f*-type atomic continua in the range from 0 to +1.8 a.u. with a step of 0.2 a.u. This basis set produces 200 discretized states per eV for the continua. To decrease the number of matrix elements, basis functions were transformed into symmetry-adapted orbitals prior to orthogonalization [19]. All DV X $\alpha$  calculations were performed with a computer program called SCAT [9, 10, 19, 20].

In DV X $\alpha$  theory, transition energies are obtainable

with the so-called transition state method [8]. The oscillator strength for every electronic transition was calculated using a dipole approximation. Numerical integrations for dipole matrix elements were performed in the manner described in Refs. [21] and [22]. Lorentzian curves with a width (FWHM) of 2.0 eV were used to reproduce observed band shapes. Although the discretized states depend on the choice of the basis set, the resultant spectrum is practically independent of the choice. This was confirmed by varying the size of the basis set.

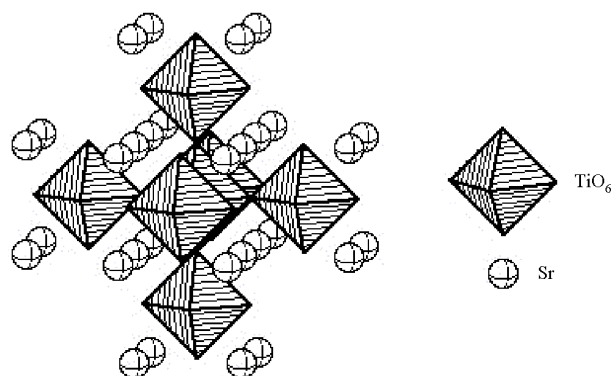


Figure 1.  $[\text{TiO}_6\text{Sr}_8(\text{TiO}_5)_6\text{Sr}_{24}]^{20+}$ , a model cluster for  $\text{SrTiO}_3$ .

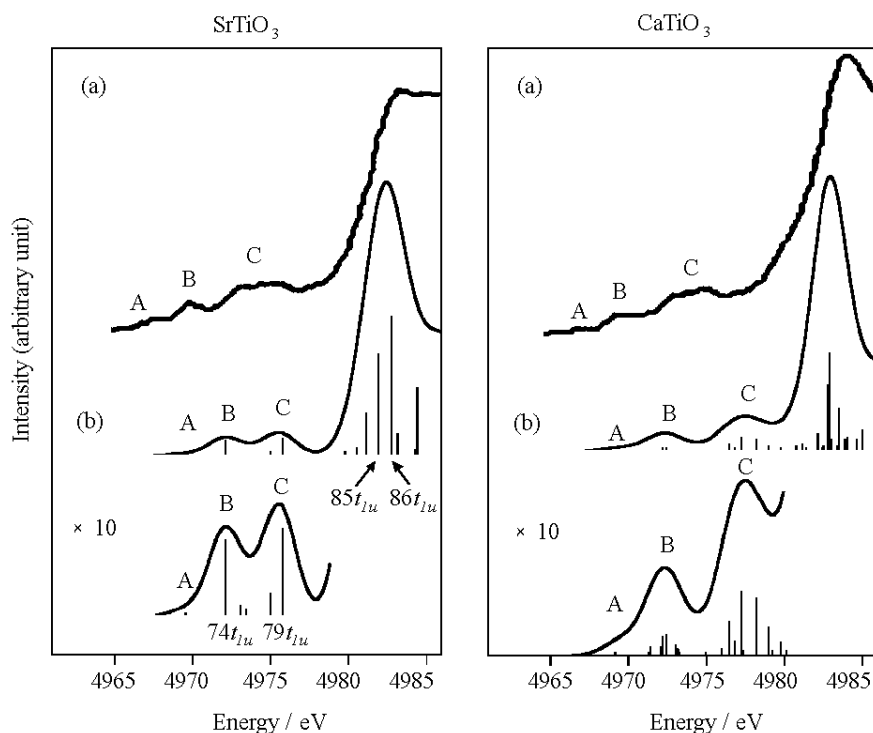


Figure 2. Observed (a) and calculated (b) Ti-K XANES spectra for  $\text{SrTiO}_3$  and  $\text{CaTiO}_3$ . Observed spectra were taken from Refs. [5] and [6]. Calculated Ti-K XANES spectra were obtained using  $[\text{TiO}_6\text{Sr}_8(\text{TiO}_5)_6\text{Sr}_{24}]^{20+}$  and  $[\text{TiO}_6\text{Ca}_8(\text{TiO}_5)_6\text{Ca}_{24}]^{20+}$  clusters. Each vertical bar is proportional to the oscillator strength for the transition to the L<sup>2</sup> state.

A  $[\text{TiO}_6\text{Sr}_8(\text{TiO}_5)_6\text{Sr}_{24}]^{20+}$  cluster in  $O_h$  symmetry was used as a model cluster for the  $\text{SrTiO}_3$  crystal. The arrangement of atoms in this cluster is shown in Figure 1, in which a central Ti atom is surrounded by an  $O_6$  octahedron, an  $\text{Sr}_8$  cube, six octahedrally coordinated  $\text{TiO}_5$  units, and then the outermost  $\text{Sr}_{24}$  shell. The Ti-O distance was taken to be 1.952 Å [23]. For  $\text{CaTiO}_3$  an analogous model cluster,  $[\text{TiO}_6\text{Ca}_8(\text{TiO}_5)_6\text{Ca}_{24}]^{20+}$ , was employed but the symmetry was somewhat reduced to  $D_{2h}$  [19]. Slater exchange scaling factor  $\alpha$  was set at 0.70.

### 3 Results and discussion

Observed (a) and calculated (b) XANES spectra for  $\text{SrTiO}_3$  and  $\text{CaTiO}_3$  are compared in Figure 2, in which the calculated spectrum was displaced in such a manner that the calculated position of the main peak comes to the observed one. In fact, it is very difficult to predict transition energies accurately in such a high-energy region. In general, two or three weak pre-edge peaks precede the main peak in the XANES spectra of titanate perovskites [2, 3]. In the case of  $\text{SrTiO}_3$  and  $\text{CaTiO}_3$  peak A is almost missing.

It is noteworthy that DV  $X\alpha$  theory reproduces fairly well the relative positions and intensities of the main and pre-edge peaks in  $\text{SrTiO}_3$  and  $\text{CaTiO}_3$ . All these peaks arise from the transitions from the  $1s$  AO of the central titanium atom. Pre-edge peaks are denoted by A, B, and C in order of increasing energy [6]. For simplicity, final states of the transitions that give rise to peaks A, B, and C will be referred to as states A, B, and C, respectively. We then examine wave functions in some detail to characterize such low-energy peaks in XANES spectra of  $\text{SrTiO}_3$ .

Figure 3 shows the profiles of representative wave functions along the O-Ti-O axis of  $[\text{TiO}_6\text{Sr}_8(\text{TiO}_5)_6\text{Sr}_{24}]^{20+}$ , a model cluster for  $\text{SrTiO}_3$ . Note that this cluster is much larger than the 51-atom cluster employed by Vedrinskii *et al.* [6]. The main peak is then attributable primarily to two  $1s$ -electron transitions. As shown in Figures 3a and 3b, the wave functions responsible for them,  $85t_{1u}$  and  $86t_{1u}$ , consist of the central titanium  $p$ -type AOs and surrounding oxygen  $p$ - and/or  $s$ -type AOs. Since the titanium  $p$ -type AOs contribute significantly to the entire wave functions, these transitions are supposed to give rise to a large overall oscillator strength. This assignment is consistent with that of Vedrinskii *et al.* [6].

Vedrinskii *et al.* suggested that peaks A and B might correspond to the splitting of surrounding titanium  $3d$  AOs into  $t_{2g}$  and  $e_g$  groups due to the octahedral crystal field, respectively [6]. This aspect of the transitions was confirmed by the present DV- $X\alpha$  calculations. However, the transition associated with peak A proved to be dipole-forbidden since the central titanium atom contributes  $3d$

AOs to state A. This is in accord with the negligibly small peak intensity. In general, even if the lowest-energy transition is symmetry-forbidden, it is often observed as a weak absorption band (e.g., the first absorption band of benzene). There is some possibility that peak A is associated with a quadrupole transition [6].

When studying the XANES spectra of a series of titanates, Vedrinskii *et al.* [6] interpreted peak B or the like as a  $1s$ -electron transition to the state (state B) in which  $p$ - and  $d$ -type AOs of the central titanium atom are hybridized due to the displacement of titanium atoms. This interpretation is apparently applicable to the spectra of  $\text{CaTiO}_3$  and  $\text{BaTiO}_3$ , in which every titanium atom is displaced from the center of an  $O_6$  octahedron. In fact, the intensity of peak B increases with increasing displacement of titanium atoms. However, peak B likewise appears in the spectra of titanates in  $O_h$  symmetry, such as  $\text{SrTiO}_3$ . Our DV  $X\alpha$  calculations with a very large basis set revealed that no displacement of titanium atoms is necessary to make peak B appreciably observable. As shown in Figure 3c, the  $p$  component of the central titanium atom is mixed with the  $d$  component of surrounding titanium atoms.

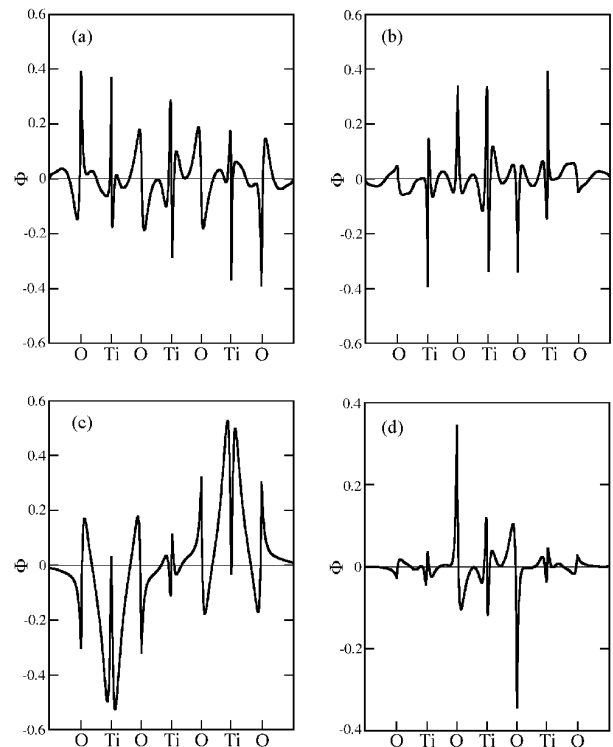


Figure 3. Views along the O-Ti-O axis of the wave functions of the  $[\text{TiO}_6\text{Sr}_8(\text{TiO}_5)_6\text{Sr}_{24}]^{20+}$  cluster corresponding to the low-energy peaks of  $\text{SrTiO}_3$ . (a)  $85t_{1u}$  for the main peak, (b)  $86t_{1u}$  for the main peak, (c)  $74t_{1u}$  for peak B, and (d)  $79t_{1u}$  for peak C.

According to Vedrinskii *et al.* [6], peak C corresponds to an interatomic transition from the central titanium to the surrounding titanium AOs. However, such a transition is unlikely to occur because the two wave functions concerned scarcely overlap. Note that the initial state is a titanium  $1s$  AO localized in the very small K shell and that the shortest Ti-Ti distance is as large as 3.91 Å for SrTiO<sub>3</sub> [19]. Therefore, the oscillator strength would not be large even if the transition occurs at all. As shown in Figure 3d, state C is a quasi-bound state that combines the  $p$  component of the central titanium atom with the  $p$  component of the surrounding oxygen atoms. The weight of the central titanium AOs in states B and C is obviously small, which makes pre-edge peaks B and C weak as compared to the main peak.

In order to make sure that peak C is not attributable to the transitions to the surrounding titanium AOs, we examined the transitions expected for a smaller [TiO<sub>6</sub>Sr<sub>8</sub>]<sup>8+</sup> cluster. This cluster represents the unit lattice of the SrTiO<sub>3</sub> crystal, in which the central titanium atom is not surrounded by other titanium atoms. In Figure 4 the calculated Ti-K XANES spectrum for [TiO<sub>6</sub>Sr<sub>8</sub>(TiO<sub>5</sub>)<sub>6</sub>Sr<sub>24</sub>]<sup>20+</sup> (a) is compared with that for [TiO<sub>6</sub>Sr<sub>8</sub>]<sup>8+</sup> (b). As in Figure 1, the calculated spectrum of [TiO<sub>6</sub>Sr<sub>8</sub>]<sup>8+</sup> was displaced in such a manner that the calculated position of the main peak comes to

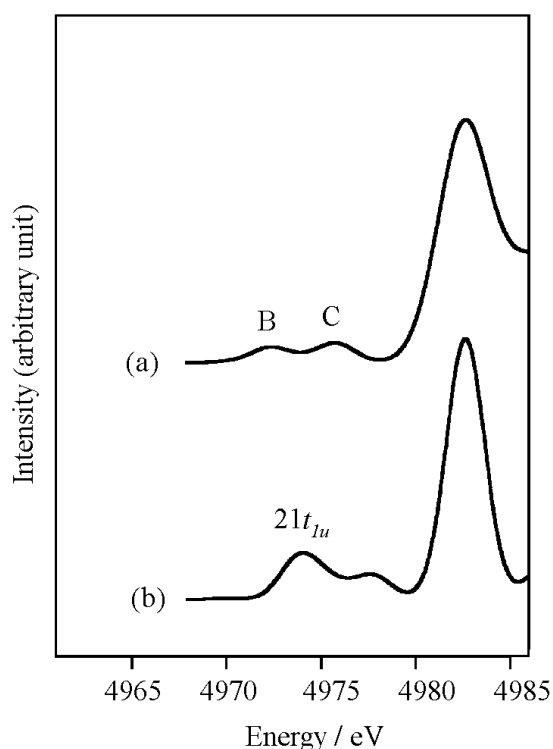


Figure 4. Calculated Ti-K XANES spectra for the central titanium atoms of [TiO<sub>6</sub>Sr<sub>8</sub>(TiO<sub>5</sub>)<sub>6</sub>Sr<sub>24</sub>]<sup>20+</sup> and [TiO<sub>6</sub>Sr<sub>8</sub>]<sup>8+</sup>.

the observed one in the SrTiO<sub>3</sub> crystal. The pre-edge structure for [TiO<sub>6</sub>Sr<sub>8</sub>]<sup>8+</sup> differs greatly from that for [TiO<sub>6</sub>Sr<sub>8</sub>(TiO<sub>5</sub>)<sub>6</sub>Sr<sub>24</sub>]<sup>20+</sup>.

In the calculated XANES spectrum of [TiO<sub>6</sub>Sr<sub>8</sub>]<sup>8+</sup>, a small peak appears midway in energy between peaks B and C for [TiO<sub>6</sub>Sr<sub>8</sub>(TiO<sub>5</sub>)<sub>6</sub>Sr<sub>24</sub>]<sup>20+</sup>. A profile of the  $21t_{2u}$  wave function corresponding to this transition is given in Figure 5, which represents a quasi-bound state that combines the  $p$  component of a central titanium atom with the  $s$  component of a neighboring oxygen atom. Since this wave function is very similar to the wave function  $79t_{1u}$  for state C in [TiO<sub>6</sub>Sr<sub>8</sub>(TiO<sub>5</sub>)<sub>6</sub>Sr<sub>24</sub>]<sup>20+</sup> (Figure 3d), it is highly probable that the former wave function represents something like state C. One should note that even a small cluster without surrounding titanium atoms generates peak C. Therefore, peak C cannot be attributed to a transition to the surrounding titanium AOs. However, the small [TiO<sub>6</sub>Sr<sub>8</sub>]<sup>8+</sup> cluster does not generate anything like state B (Figure 4b). This supports the view that peak B does not appear without surrounding titanium atoms.

As shown in Figure 1, the number of non-degenerate states for CaTiO<sub>3</sub> is larger than that for SrTiO<sub>3</sub> since the model cluster for CaTiO<sub>3</sub> has lower symmetry ( $D_{2h}$ ). However, the above assignments of the main peak and pre-edge peaks A, B, and C for SrTiO<sub>3</sub> in principle apply to the assignments of low-energy peaks in CaTiO<sub>3</sub>.

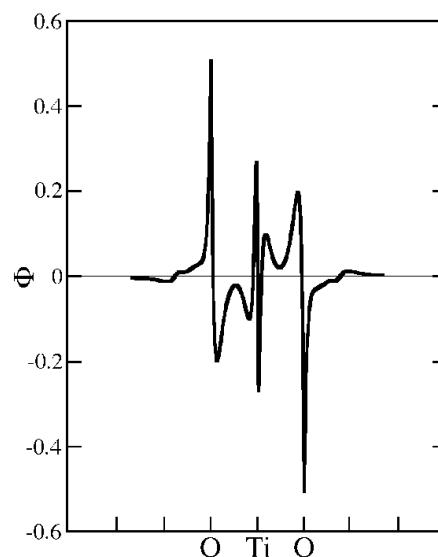


Figure 5. View of the wave function  $21t_{2u}$  of [TiO<sub>6</sub>Sr<sub>8</sub>]<sup>8+</sup> along the O-Ti-O axis.

## 4 Concluding Remarks

We successfully made assignments of typical low-energy peaks in the Ti-K XANES spectrum of SrTiO<sub>3</sub> using the DV X $\alpha$  cluster model combined with L<sup>2</sup> continuum wave functions. All the peaks were attributed consistently to the dipole-allowed 1s-electron transitions to the p-type AOs of the same titanium atom. Deformation of the lattice was not required to attribute the observed peaks to the dipole-allowed transitions. Assignments made by Vedrinskii *et al.* [6] are different in these respects. Satisfactory agreement between observed and calculated spectral features suggests that we have used right molecular orbital theory together with a sufficiently large basis set and a sufficiently large model cluster.

As has been seen, our DV-X $\alpha$  cluster method has an advantage in that it can utilize a very large basis set, which can generate wave functions that cover a very large energy range. Such wave functions indeed are needed to analyze XANES spectra. The X $\alpha$  potential is much more realistic than the muffin-tin potential often used in the MS method. Although the formal charge of +20 in the [TiO<sub>6</sub>Sr<sub>8</sub>(TiO<sub>5</sub>)<sub>6</sub>Sr<sub>24</sub>]<sup>20+</sup> model cluster may be very large, it presumably produces a fairly small effect on the transition energies within the cluster. Band theory has not been a popular tool for characterizing XANES transitions because they are not ordinary band-to-band transitions. Furthermore, it is not easy to include the effect of hole formation on the X-ray absorption spectra in band theory.

This work was supported by a Sasakawa Scientific Research Grant from the Japan Science Society. Computations were carried out at the Information Processing Center, Shizuoka University.

## References

- [1] J. Stohr, *NEXAFS Spectroscopy*, Springer-Verlag, Berlin (1992).
- [2] B. Ravel, E. A. Stern, Y. Yacobi, and F. Dogan, *Jpn. J. Appl. Phys., Suppl.*, **32-2**, 782 (1993).
- [3] B. Ravel and E. A. Stern, *Physica B*, **208-209**, 316 (1995).
- [4] C. Bouldin, J. Sims, H. Hung, J. J. Rehr, and A. L. Ankudinov, *X-Ray Spectrom.*, **30**, 431 (2001).
- [5] A. L. Ankudinov, B. Ravel, J. J. Rehr, and S. D. Conradson, *Phys. Rev. B*, **58**, 7565 (1998).
- [6] R. V. Vedrinskii, V. L. Kraizman, A. A. Novakovich, Ph. V. Demekhin, and S. V. Urazhdin, *J. Phys.: Condens. Matter*, **10**, 9561 (1998).
- [7] Z. Y. Wu, G. Ouvrard, P. Gressier, and C. R. Natoli, *Phys. Rev. B*, **55**, 382 (1997).
- [8] H. Nakamatsu, T. Mukoyama, and H. Adachi, *Chem. Phys.*, **143**, 221 (1990).
- [9] H. Nakamatsu, T. Mukoyama, and H. Adachi, *Jpn. J. Appl. Phys., Suppl.*, **32-2**, 23 (1993).
- [10] H. Nakamatsu, H. Adachi, and T. Mukoyama, *Bull. Inst. Chem. Res. Kyoto Univ.*, **72**, 45 (1994).
- [11] H. Nakamatsu and T. Mukoyama, *J. Chem. Phys.*, **95**, 3167 (1991).
- [12] H. Nakamatsu and T. Mukoyama, *Adv. Quantum Chem.*, **37**, 111 (1999).
- [13] M. Uda, D. Yamashita, D. Terashi, T. Yamamoto, H. Osawa, K. Kanai, H. Nakamatsu, and R. Perera, *J. Elec. Spectrosc. Relat. Phenom.*, **114-116**, 819 (2001).
- [14] J. Tsuji, K. Kojima, S. Ikeda, H. Nakamatsu, T. Mukoyama, and K. Taniguchi, *J. Synchrotron Rad.*, **8**, 554 (2001).
- [15] H. Adachi, M. Tsukada, and C. Satoko, *J. Phys. Soc. Jpn.*, **45**, 875 (1978).
- [16] P. W. Langhoff, *Chem. Phys. Lett.*, **22**, 60 (1973).
- [17] P. W. Langhoff, J. Sims, and C. T. Corcoran, *Phys. Rev. A*, **10**, 829 (1974).
- [18] W. P. Reinhardt, *Comput. Phys. Commun.*, **17**, 1 (1979).
- [19] H. Nakamatsu, *Chem. Phys.*, **200**, 49 (1995).
- [20] H. Adachi, M. Tsukada, and C. Satoko, *J. Phys. Soc. Jpn.*, **45**, 875 (1978).
- [21] H. Adachi and K. Taniguchi, *J. Phys. Soc. Jpn.*, **49**, 1944 (1980).
- [22] B. Song, H. Nakamatsu, R. Sekine, T. Mukoyama, and K. Taniguchi, *J. Phys.: Condens. Matter*, **10**, 9443 (1998).
- [23] K.-H. Hellwege, ed., *Landolt-Börnstein, New Series, Group III, Vol. 16*, K.-H. Hellwege, Springer-Verlag, Berlin (1981), p. 58.

# SrTiO<sub>3</sub> と CaTiO<sub>3</sub> の Ti-K XANES スペクトルにおける 低エネルギーピークの起源

藤田 昌樹<sup>a</sup>, 中松 博英<sup>b</sup>, 杉原 淳<sup>c</sup>, 相原 惇一<sup>a</sup>, 関根 理香<sup>a\*</sup>

<sup>a</sup> 静岡大学理学部化学科, 〒 422-8529 静岡県静岡市大谷 836

<sup>b</sup> 京都大学化学研究所, 〒 611-0011 京都府宇治市五ヶ庄

<sup>c</sup> 湘南工科大学材料工学科, 〒 251-8511 神奈川県藤沢市辻堂西海岸 1-1-25

\*e-mail: scrseki@ipc.shizuoka.ac.jp

SrTiO<sub>3</sub> と CaTiO<sub>3</sub> の Ti-K XANES スペクトルの低エネルギー部分はメインピークと吸収端前ピーク B、C からなる。われわれは L<sup>2</sup> 連続状態波動関数を取り入れた DV X $\alpha$  法を用いて、これらのピークの帰属を行った。この DV X $\alpha$  法をモデルクラスター [TiO<sub>6</sub>M<sub>8</sub>(TiO<sub>5</sub>)<sub>6</sub>M<sub>24</sub>]<sup>20+</sup> ( M=Sr または Ca ) に適用することにより、これらのピークの相対位置と強度を再現することに成功した。これらのピークはすべて、チタン原子の 1s 電子から同じチタン原子の p 型原子軌道関数 (AO) への遷移であることがわかった。一般に、モデルクラスターの中心のチタン原子の p 型 AO はその周囲の原子のさまざまな AO と混合する。このように、典型的なペロブスカイト型チタン酸塩である SrTiO<sub>3</sub> と CaTiO<sub>3</sub> のメインピークと吸収端前ピークの起源を単一の理論的枠組みの中で矛盾なく説明することができた。

キーワード: XANES, 吸収端前ピーク, チタン酸ストロンチウム, チタン酸カルシウム, DV X $\alpha$  法